NJC

Accepted Manuscript

This is an *Accepted Manuscript*, which has been through the Royal Society of Chemistry peer review process and has been accepted for publication.

Accepted Manuscripts are published online shortly after acceptance, before technical editing, formatting and proof reading. Using this free service, authors can make their results available to the community, in citable form, before we publish the edited article. We will replace this *Accepted Manuscript* with the edited and formatted *Advance Article* as soon as it is available.

You can find more information about *Accepted Manuscripts* in the Information for Authors.

Please note that technical editing may introduce minor changes to the text and/or graphics, which may alter content. The journal's standard Terms & Conditions and the Ethical guidelines still apply. In no event shall the Royal Society of Chemistry be held responsible for any errors or omissions in this *Accepted Manuscript* or any consequences arising from the use of any information it contains.

ROYAL SOCIETY OF CHEMISTRY

www.rsc.org/njc

Journal Name

RSCPublishing

ARTICLE

Two Novel Cyanido-Bridged Polymeric Complexes with Suspension Bridge Type Connections and a Series of Related Complex Salts: Crystallographic and Thermal Characterizations

Cite this: DOI: 10.1039/x0xx00000x

Received 00th.....2014,
Accepted 00th.....2014

DOI: 10.1039/x0xx00000x

www.rsc.org/

Aysegul Şenocak,[a] Ahmet Karadağ,[a]* Mustafa Serkan Soylu,[b] Ömer Andaç[c]

In this study, two cyanido-bridged coordination polymers and three cyanido complex salts with general formulas of [M(*edbea*)Ni(CN)$_4$] {M= Zn (**1**), Cd (**2**); *edbea*= 2,2′-(ethylenedioxy)bis(ethylamine)} and [Cd(*edbea*)$_2$][M′(CN)$_4$].XH$_2$O {(M′= Ni (**3**), Pd (**4**), Pt (**5**); X= 2 (**3**), 0 (**4** and **5**)} were synthesized and characterized with elemental analysis and *FT-IR* spectroscopy. *X*-ray studies of **1**-**5** exhibited two different coordination modes of *edbea* ancillary ligand. While *edbea* acts as a suspension bridge with two nitrogen atoms in an unusual way between adjacent metal ions for **1** and **2**, in the remaining complexes, it behaves tetradentate ligand by ending up with eight coordinated Cd^{II} center. **3** showed an interesting packing of the cationic portions hosted between the layers created by the anions and lattice waters. Thermal analysis studies showed that all complexes exhibited similar mechanism in which neutral groups were released, first and then, anionic ligands decomposed. Also, the complexes with salt structure could not remain their thermal stability as long as polymeric ones.

INTRODUCTION

Coordination complexes exhibit immense commercial applications, ranging from metallodrugs in medicine to agents for metal extraction from ores. Metallodrugs, which have been used for bioassay, diagnostic imaging, anticancer drugs, arthritis, diabetes,…etc. Nowadays, have a history of thousands of years old. Detection of a metal ion or alternatively a ligand species is carried out by formation of coordination compounds depending on selective binding. The synthetic chemical industry massively depends on metal complexes as catalysts. Jacobsen catalyst and Wilkinson's catalyst are some of them. Metal complexes, especially polymetallic systems, within the size range of 1-100 nm, can be used as a starting point for nanomaterials. By using selective complexation, extraction of the contaminating metals from the soil is carried out.[1]

One of the most known classes of coordination complexes is coordination polymers. On the purpose of formation of coordination polymers, the key is selection of bridging ligands. For this aim, cyanido ligand is widely used.[2-8] The most eye-catching characteristic of cyanido ligand is to coordinate either as terminal or bridging ligand.[9] Cyanidometallates are one of the most extensively used building blocks capitalizing on the coordination ability of the cyanido group to bridge two metal ions.[10] Besides, cyanido group exhibits polar character and forms hydrogen bonds (HBs) resulting in more stable structures.[11]

Cyanido complexes are a class of compound maintaining its importance at the present time because of a great variety of using areas. Studies on cyanido complexes have especially focused on paramagnetic centered ones (Fe, Co and Mn,… etc.) which are used to prepare molecule-based magnetic materials.[12-16] This extensive interest resulted in Zn and Cd centered cyanido complexes that are ignored their importance. These complexes have not taken enough attention in spite of their interesting structural patterns. For example; binuclear Zn units are bridged via tetracyanopalladate building blocks in a polymeric complex with general formula of $[Zn_2[OH(CH_2)_2NH(CH_2)_2NH(CH_2)_2OH]_2Pd(CN)_4]$.[17] Similar type bridge formation are observed in two Zn^{II} complex structures in the literature.[18,19] Besides, in a study carried out by Kurkcuoglu and co-workers, non-covalent Ni(II)…π binding forces, very important in stabilizing of the polymeric structure, are observed.[20]

Edbea {2,2'-(Ethylenedioxy)bis(ethylamine); alternatively named 2-[2-(2-aminoethoxy)ethoxy]ethanamine or 1,8-diamino-3,6-dioxaoctane; $H_2N(CH_2)_2O(CH_2)_2O(CH_2)_2NH_2$} is used in this study as a co-ligand which have four donor atoms. This ligand has not been used as a ligand for synthesis of coordination complexes, commonly in spite of plentifulness of its donor atoms. *Edbea* was chosen as co-ligand because of possible interesting complex structures originating from its linear geometry and four donor atoms. In the literature, *edbea* ligand can coordinate as a bidentate ligand through two donor atoms (*N* and *N*′) (in this study) or it can use all donor atoms for coordination. In the second situation, whether *edbea* can coordinate to only one metal ion by using four donor atoms (in this study) or it can form bridge between two metal ions.[21] Besides, there are some complex structures with *edbea* ligand whose structure could not be illuminated by *X*-ray single crystal method.[22]

In this paper, we reported the synthesis, *FT-IR* spectra and thermal analyses of five new heteronuclear cyanido-complexes. Also, *X*-ray single crystal structures of **1**-**4** and powder crystal structure of **5** were determined. While the complex structures of **1** and **2** were cyanido-bridged coordination polymers, the remaining complexes (**3-5**) were composed of complex ions. Especially, **1** and **2** had quite interesting secondary bridge structures in addition to cyanido bridges. *Edbea* co-ligand, occasionally used as ligand without modification, has formed chelate complexes by using all donor atoms.[23-24] However, it coordinated via only -N and -N′ donor atoms to same kind neighbor

metal centers in the chain structure of **1** and **2**. By this way, an interesting suspension bridge formation was observed for aforesaid complexes. As for other complexes, a cyanidometallate ion and a cationic unit, forming by coordination of two *edbea* ligand to Cd^{II} ion, originated a salt structure.

RESULTS and DISCUSSION

As a continuation of an ongoing research, we investigated the reactions of $[Ni(CN)_4]^{II}$ with Zn^{II} and Cd^{II} metal ions and *edbea* co-ligand. Zn^{II} formed only polymeric cyano-bridged polymeric complex at room temperature while both polymeric and monomeric structures were obtained by using Cd^{II} center metal. Thereon, the remaining members of group 10 were wondered what kind of complex structures to form. For this aim, Pd^{II} and Pt^{II} metal ions were used for synthesis of Cd complexes instead of Ni^{II} and, obtained products were characterized by using various spectroscopic methods in this study.

X-Ray Single Crystal Structures

Crystal Structures of 1 and 2. Complexes **1** and **2** crystallized in the orthorhombic space group *Pbcn* and monoclinic space group C2/c, respectively. An amazing aspect of these complexes was that *edbea* bonds together Zn^{II} or Cd^{II} centers just like a suspension bridge. The *1D* chain of **1** consisted of Zn^{II} centers spliced together via *edbea* bridges (Figure 1). In this chain, *edbea* acts as a suspension bridge by coordinating with its two amino groups to neighbor Zn^{II} ions. In addition to *edbea*, tetracyanidonickelate^{II} ions, using two cyanido groups for bridge formation, provided inter-chain connections resulting in *2D* planes (Figure 2a). In this *2D* chain structure, the Ni center ions were colinear at a distance of 7.372 Å. The stacking distance of these layers was 5.7315 Å (Figure 2b).

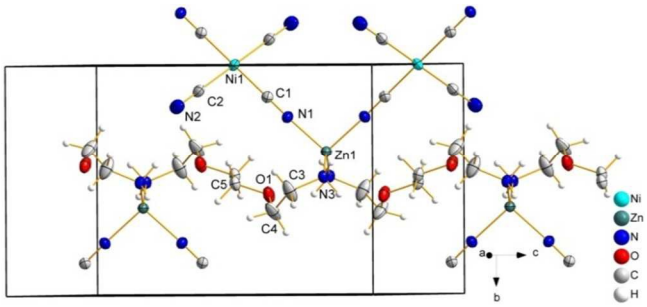

Fig 1 The *1D* chain of **1** {Catena-poly[dicyanido-1κ^{2}C-μ-cyanido-1:2κ^{2}C:N-μ-cyanido-1′:2κ^{2}C:N-μ-[2,2′(ethylenedioxy)bis(ethyl amine)-2:2′κ^{2}N:N′]-μ-[2,2′(ethylenedioxy)bis(ethylamine)-2:2″κ^2 N:N′]dizinc^{II}nickel^{II}]-μ-cyanido-1:2′κ^{2}C:N]}.

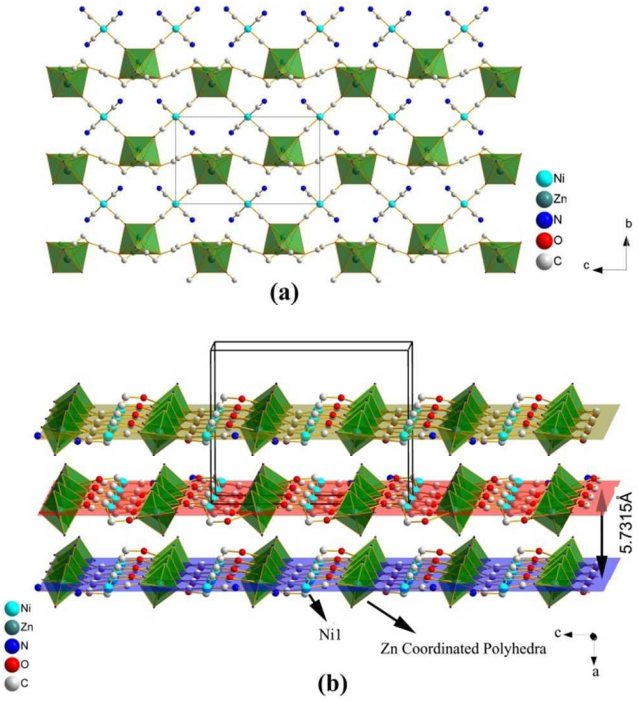

Fig 2 (a) The *2D* plane of **1**. **(b)** Assembly of *2D* planes through *b* axis of **1** (N atoms of $[Ni(CN)_4]^{2-}$ and H atoms are omitted for the clarity of the picture).

Complex **2** followed similar pattern with **1** except for coordination number of the second metal. Complex **2** exhibited same suspension bridge type binding of e*dbea* as complex **1**. As distinct from complex **1**, bridge behavior of all four cyanido groups in addition to *edbea* co-ligand resulted in *3D* network structure and Tetracyanidonickelate^{II}

ions act as a bridge between Cd atoms in the packing. (Figure 3a and b)

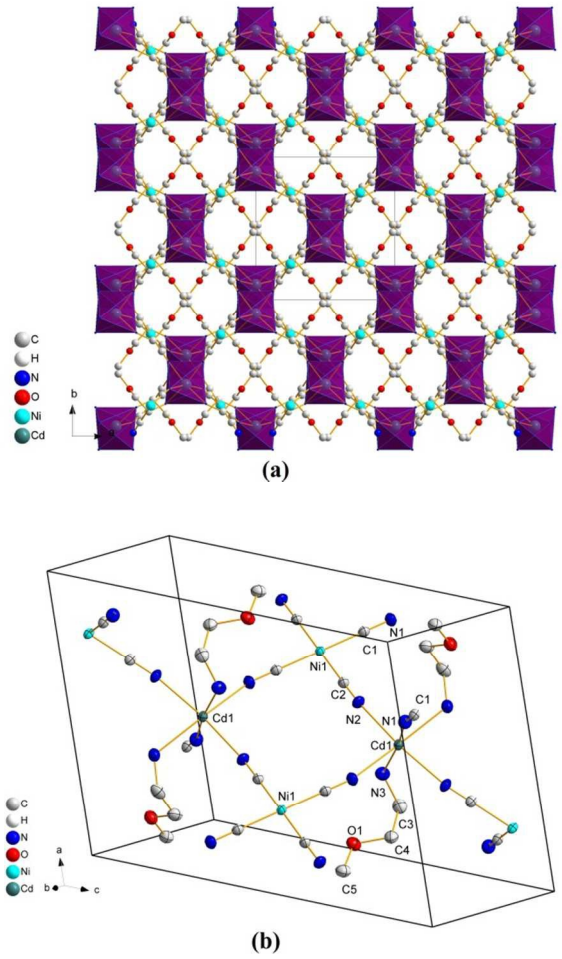

Fig 3 (a) The *3D* chain of **2**{Catena-poly[μ-cyanido-1:2′′′κ^2C:N-μ-cyanido-1:2′′′κ^2C:N-μ-cyanido-1:2κ^2C:N-μ-[2,2′-(ethylenedioxy) bis(ethylamine)-2:2′κ^2N:N′]-μ-[2,2′-(ethylenedioxy)bis(ethylamine)-2:2′′′′κ^2N:N′]dicadmium^{II}nickel^{II}]-μ-cyanido-1:2′κ^2C:N]} (H atoms are omitted for clarity). **(b)** Unit cell of **2**.

In both complexes, *edbea* undertook bridge formation duty between same metal centers. *Edbea* exposed to some deformations in comparison with original conformation of free ligand when served as a bridge in those complex structures (Figure 4). While relatively significant deformation was observed for **1**, conformation of *edbea* in **2** was quite close to that of free ligand. This difference may originate from steric hindrance occurring because of relatively smaller radius of Zn^{II} metal ion.

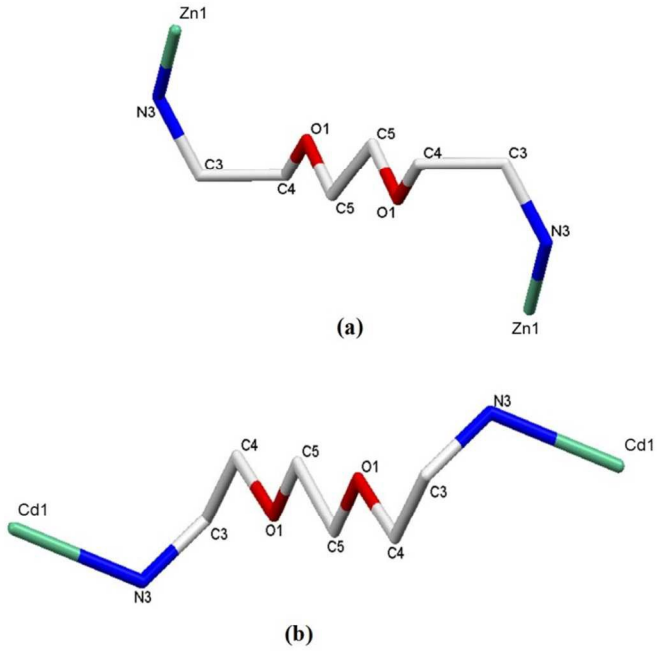

Fig 4 (a) *edbea* fragment in **1**. **(b)** *edbea* fragment in **2**.

In the anionic fragment, Ni^{II} center metal was surrounded by four cyanido carbons in square planar geometry for both complexes. While all cyanido groups acted as bridging ligands in the structure of **2**, cyanido species were in two different positions in the tetracyanidonickelate^{II} frame of **1**: terminal and bridging ligand. $[Ni(CN)_4]^{II}$ anions bonded to dimeric cationic units via bridging cyanido ligands and the formation of the *2D* or *3D* polymeric chains carried out in this way. In spite of the existence of two different type cyanido groups for **1**, bond distances observed between Ni^{II} ion and cyanido carbons were almost equal (Table 1). This situation was probably caused by the formation of *HB* between the terminal cyanido group and amino group of *edbea* ligand. Ni-C bond distances of **1** and **2** were in a good accordance with literature values.[25-32] When it comes to C-Ni-C angles, ideal values were exhibited for both complexes because of keeping ideal square planar geometry.

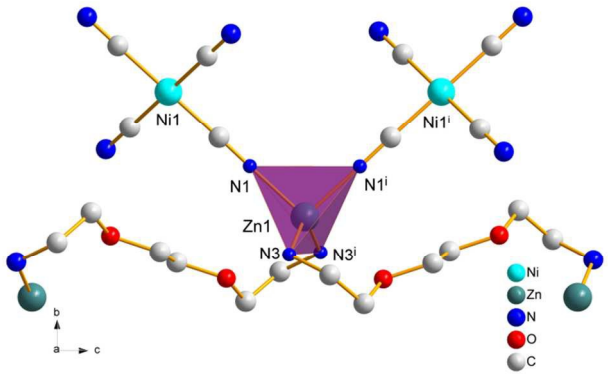

Fig 5 The coordination environment of Zn^{II} ion in **1** (H atoms are omitted for clarity) (Symmetry Code i: *1-x, y, ½-z*).

In the complex structure **1**, Zn^{II} ion was four coordinated by two cyanido nitrogens from different tetracyanidonickelates^{II} and two nitrogen atoms from different *edbea* ligands to complete a tetrahedral geometry (Figure 5). Zn-N(1) and Zn-N(3) bond distances were almost equal and a little bit shorter in comparison to literature values because of suspension bridge behavior of *edbea* ligand, probably.[20,33-36] In the coordination environment of Zn^{II} ion, deviations were observed from ideal tetrahedral geometry angle because of steric hindrance of *edbea* ligands. Angle enlargement was observed in N(3)-Zn-N(3) in consequence of big space covered by methylene groups of *edbea*. On the other hand, N(1)-Zn-N(1) angle narrowed in comparison with ideal value due to the same reason.

Table 1 Bond distances and bond angles of **1**

Bond Lengths (Å)			
Ni-C(1)	1.8535(1)	Zn-N(1)	2.0214(1)
Ni-C(2)	1.8692(1)	Zn-N(3)	2.0109(1)
Bond Angles (°)			
C(1)-Ni-C(1)	180.00	N(1)-Zn-N(1)	95.74
C(2)-Ni-C(2)	180.00	N(3)-Zn-N(3)	120.76
C(1)-Ni-C(2)	89.51	N(1)-Zn-N(3)	113.79
C(1)-Ni-C(2)	90.49	N(1)-Zn-N(3)	105.05
Ni-C(1)-N(1)	178.87	Zn-N(1)-C(1)	171.15
Ni-C(2)-N(2)	179.22		

The Cd^{II} cation is six-coordinated in an octahedral geometry defined by six nitrogen atoms from four tetracyanidonickelate^{II} anions and two different *edbea* ligands (Figure 6). While cyanido nitrogens occupied axial sites in this coordination geometry, two *edbea* nitrogens and remaining two cyanido nitrogens located in the equatorial plane in *cis*-position. While Cd-N(1) and Cd-N(2) bond lengths were almost equal, Cd-N(3) bond distance was a bit longer because of steric hindrance of methylene groups of *edbea* (Table 2). Nevertheless, all Cd−N bond lengths were within the range reported for octahedral Cd^{II} based cyanido-bridged coordination polymers.[20,34,35,37-39] When it comes to bond angles, steric bulkiness of *edbea* ligand caused deviations from ideal square planar geometry in the equatorial plane. For this reason, an expanding of N(3)-Cd-N(3) angle and narrowing of other angles in the equatorial plane were observed.

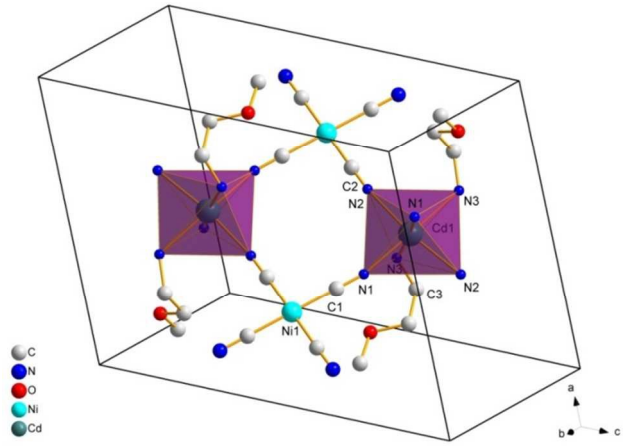

Fig 6 Polyhedral representation and the coordination environment of Cd^{II} ion in **2**.

Table 2 Bond distances and bond angles of **2**

Bond Lengths (Å)			
Ni-C(1)	1.8595(1)	Cd-N(2)	2.3419(1)
Ni-C(2)	1.8573(1)	Cd-N(3)	2.3642(1)
Cd-N(1)	2.3274(1)		
Bond Angles (°)			
C(1)-Ni-C(1)	180.00	N(2)-Cd-N(2)	165.28
C(2)-Ni-C(2)	180.00	N(3)-Cd-N(3)	107.19
C(1)-Ni-C(2)	89.91	N(2)-Cd-N(1)	98.69
C(1)-Ni-C(2)	90.09	N(2)-Cd-N(1)	92.10
Ni-C(1)-N(1)	179.62	N(2)-Cd-N(3)	90.37
Ni-C(2)-N(2)	178.88	N(2)-Cd-N(3)	80.88
N(1)-Cd-N(3)	169.30	C(1)-N(1)-Cd	166.07
N(1)-Cd-N(1)	85.86	C(2)-N(2)-Cd	163.78

For **1**, there were inter-molecular and intra-molecular *HBs*. Inter-molecular *HBs* stabilized structure by increasing the interaction between *2D* chains. When it comes to remaining *HBs*, a quite interesting formation drew attention. Amine hydrogen (H(3D)) of *edbea* ligand formed bifurcated *HB*. It was bonded both O(1) and N(2) at the same time. The reason for the formation of those *HBs* was the excess of *HB* acceptor capacity over the number of hydrogen bonding protons available.[39] As for **2**, only one inter-ligand *HB* formed (Table 3).

Better insight into the structure of the metal–organic frameworks is provided by the topological network approach, which has proved to be an important and essential aspect of the design and analysis of MOF. To further understand the structure and packing of **2**, a topological analysis was studied by using TOPOS 4.0.[40] In the studied structure, each Cd^{II} and Zn^{II} units can be regarded as 4 and 6 connected nodes respectively. And so complex **2** possess a new binodal 4,6-connected 3D-network with the point symbol of $\{4^2.5^3.7\}\{4^2.5^5.6^4.7^4\}$ (Figure 7).

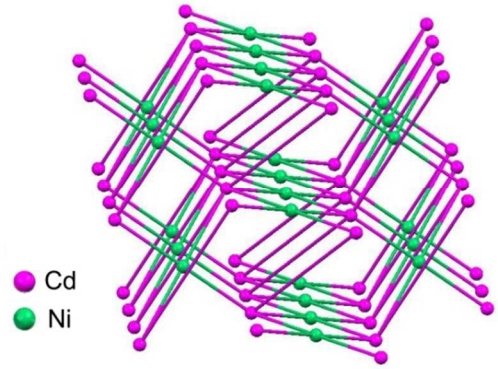

Fig 7 Representation of the new binodal 4,6 connected network with the point symbol of $\{4^2.5^3.7\}\{4^2.5^5.6^4.7^4\}$ of 2. Green and pink balls represent the Ni and Cd atoms, respectively.

It is noticed that **2** exhibits no solvent accessible voids in the crystal packing, resulting in *1D* micro channels along *a* axis. PLATON program[41] shows that the framework provides 2.1% of void space of the total crystal volume (32.7 $Å^3$ out of the 1537.5$Å^3$ unit-cell volumes) (Figure 8).

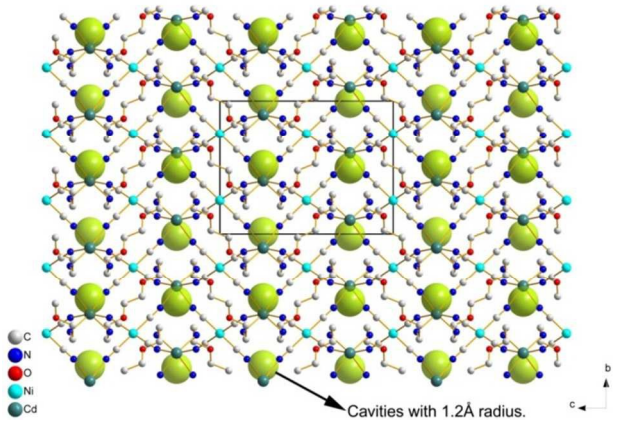

Fig 8 The non-solvent accessible volumes in **2**. The cavities represented as green balls with 1.2 Å radius.

Table 3 *HBs* data of **1** and **2**

	1			
	D–H	***H···A***	***D···A***	***D–H···A***
N(3)-H(3D)···O(1)^{i}	0.90	2.39	2.949	120
N(3)-H(3C)···N(2)^{ii}	0.90	2.16	3.040	166
N(3)-H(3D)···N(2)^{iii}	0.90	2.55	3.372	152
	2			
	D–H	***H···A***	***D···A***	***D–H···A***
N(3)-H(3D)···O(1)^{iv}	0.90	2.65	3.205	121

[i] x-1/2, -y+3/2, -z; [ii] -x+1, y, -z+1/2; [iii] -x+1, -y+1, -z; [iv] -x+1/2, -y+1/2, -z+1

Crystal Structures of 3, 4 and 5. Single crystal *X*-ray structural study revealed that **3** and **4** salts with the general formula of $[Cd(edbea)_2][M'(CN)_4].XH_2O$ [M′= Ni^{II} and X= 2 for **3**, M′= Pd^{II} and X= 0 for **4**] crystallized in orthorhombic and monoclinic crystal systems, respectively. Their structures were successfully solved and converged in the space group $P2_1$ and C2/c, respectively. Powder X-ray study of **5** revealed that **4** and **5** are isomorphous (Fig 9 and 10). **3**, **4** and **5** can be said to exhibit same molecular structure except for lattice water in the structure of **3**. All three complexes had one anionic unit with square planar geometry and one cationic unit which have eight-coordinated structure. While Ni^{II} cations were surrounded by four cyanido carbon in **3**, cationic unit formed by coordination of four nitrogen and four oxygen atoms from two *edbea* ligands using all donor atoms (Figure 11).

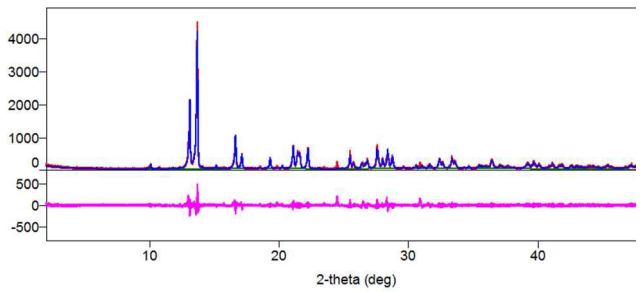

Fig 9 Observed (red), calculated (blue) and residual *X*-ray powder data for **5**.

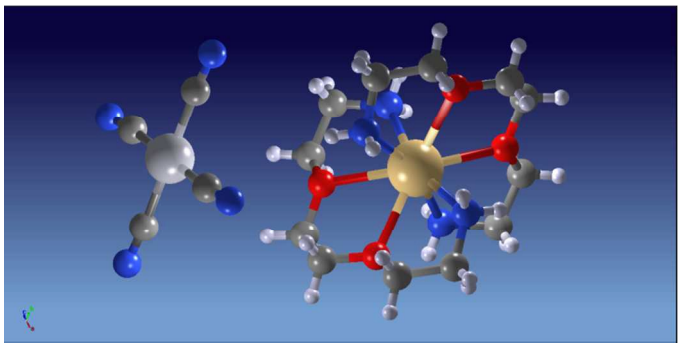

Fig 10 *X*-ray powder structure for **5**.

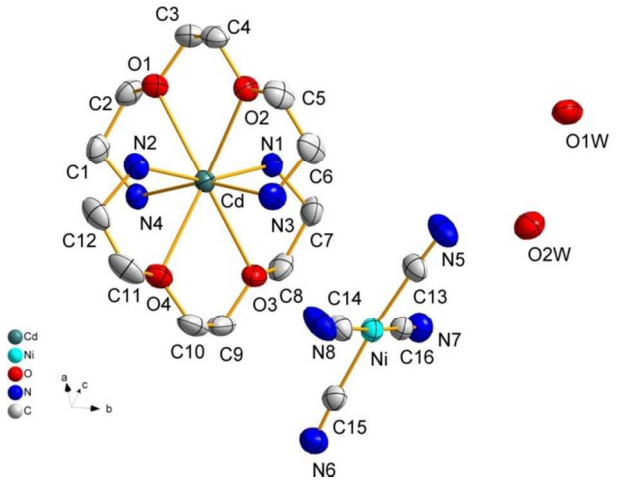

Fig 11 The molecular structure and atom numbering scheme of **3** (The hydrogen atoms are hidden in terms of clarity of figure).

Ni^{II} ion had square planar $Ni^{II}C4$ coordination with ligation of carbon atoms from four cyanido ligands (Ni^{II}-C= 1.855(5)-1.874(5) Å). The bond distances resulting from those coordinations were a little bit different from each other because of different locations and interactions of cyanido ligands (Table 4). After all, whole coordination bond distances in the coordination environment of Ni^{II} fell within the range observed for Ni^{II} based coordination polymers.[42-48] When it comes to bond angles, little deviations from ideal linear angles were observed especially at the cyanido groups near to lattice waters. These deviations probably spring from locations of cyanido ligands with regards to lattice waters and *edbea* ligands.

Table 4 Bond distances and bond angles for **3**

Bond Lengths (Å)			
Ni-C(13)	1.860(5)	Cd-N(3)	2.388(4)
Ni-C(14)	1.855(5)	Cd-N(4)	2.378(3)
Ni-C(15)	1.874(5)	Cd-O(1)	2.639(3)
Ni-C(16)	1.864(5)	Cd-O(2)	2.542(3)
Cd-N(1)	2.336(3)	Cd-O(3)	2.624(3)
Cd-N(2)	2.328(3)	Cd-O(4)	2.577(3)
Bond Angles (°)			
C(13)-Ni-C(15)	174.9(2)	N(4)-Cd-N(3)	163.03(1)
C(14)-Ni-C(16)	176.2(2)	O(2)-Cd-O(4)	145.07(9)
C(13)-Ni-C(14)	88.35(2)	N(2)-Cd-O(3)	130.11(1)
C(14)-Ni-C(15)	91.96(2)	N(1)-Cd-N(3)	95.51(1)
Ni-C(13)-N(5)	176.0(5)	N(2)-Cd-N(4)	93.81(1)
Ni-C(14)-N(8)	176.5(5)	N(2)-Cd-N(3)	88.62(1)
Ni-C(15)-N(6)	176.7(4)	N(2)-Cd-O(2)	84.08(1)
Ni-C(16)-N(7)	179.0(4)	N(3)-Cd-O(3)	77.65(1)
N(2)-Cd-O(4)	69.87(1)	O(4)-Cd-O(3)	61.92(1)
O(2)-Cd-O(1)	61.55(9)		

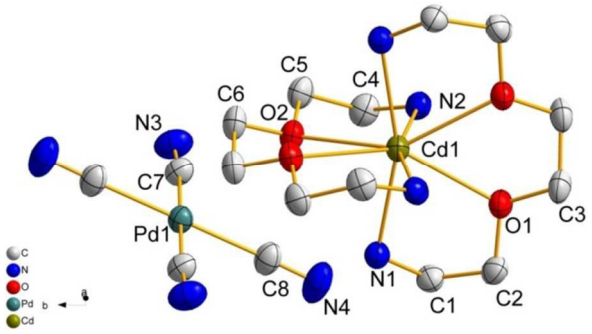

Fig 12 The molecular structure of **4**.

In analogy to **3**, **4** had an anionic unit which has a square planar arrangement around a palladium center (Figure 12). In this complex structure, Pd-C bond distances were almost of the same value and similar to those of the previously reported tetracyanopalladate^{II} complexes (Table 5).[34,49-52] The C-Pd-C bond angles, which are equal to 180°, indicated that the complex retained original square planar geometry probably because of absence of lattice water. The Pd-C-N angles exhibited somewhat deviation from ideal value.

Table 5 Bond distances and bond angles for **4**

Bond Lengths (Å)			
Pd(1)-C(7)	1.990(7)	Cd(1)-N(2)	2.346(5)
Pd(1)-C(8)	1.996(4)	Cd(1)-O(1)	2.508(2)
Cd(1)-N(1)	2.408(3)	Cd(1)-O(2)	2.577(3)
Bond Angles (°)			
C(7)-Pd-C(7)	180.00	O(1)-Cd-O(1)	63.11(12)
C(7)-Pd-C(8)	94.4(2)	N(1)-Cd-N(2)	93.39(11)
C(7)-Pd-C(8)	85.6(2)	N(1)-Cd-N(2)	89.75(11)
Pd-C(7)-N(3)	174.7(4)	N(1)-Cd-N(1)	161.52(10)
Pd-C(8)-N(4)	175.4(7)	N(2)-Cd-N(2)	160.37(16)
O(2)-Cd-O(2)	63.46(12)		

Cd^{II} ion was eight coordinated with four nitrogen and four oxygen atoms from two *edbea* ligands in both complexes. *Edbea* ligands were located in perpendicular positions to each other to minimize

steric hindrance (Figures 13 and 14). In order to clarify the geometry of eight-coordinated metal centers, several methods have been used. Burdett et all. had analyzed eight-coordinated molecules in all possible geometries (dodecahedron, square antiprism, bicappedtrigonal prism, cube, hexagonal bipyramid, square prism, bicappedtrigonalantiprism).[53] Muetterties and Wright had reported that the structures with dodecahedron, square antiprism and bicappedtrigonal prism were low-energy structures.[54] Haigh had advised a simple criterion for distinguishing the types of low-energy structures.[55] In accordance with Haigh, Cd^{II} ions in **3** and **4** were determined to have triangular dodecahedron geometry because of being close together of the 16th, 17th and 18th lowest L-Cd-L' angles (88.62, 93.81 and 95.51° for **3**; 89.75, 93.39 and 93.39° for **4**). Another method was suggested by Xu et all. using their Matlab® code.[56]

$$S=\min\left[\frac{1}{m}\sqrt{\sum_{i=1}^{m}(\delta_i-\theta_i)^2}\right]$$

Where m= number of edges, δ= angle between normals of adjacent faces, δ_i= observed dihedral angle along the i^{th} edge of δ, and θ= same angle of corresponding ideal polytopal shape. The smallest S value is the one closest to describing the coordination geometry. Atomic coordinates used for shape measure calculation were given in Table 6. The shape measure S(°) were calculated as 39.34° and 27.43° for trigonal dodecahedron (D_{2d}), 39.04° and 25.98° for bicappedtrigonal prism (C_{2v}), 41.74° and 29.35° for square antiprism (D_{4d}) for **3** and **4**, respectively. Shape measure results did not correlate the results found by Haigh's criteria. The lower shape measure showed that the coordination polyhedron for both complexes was closest to the bicappedtrigonal prism or hendecahedron.

Table 6 Atomic coordinates used for shape measure for **3** and **4**

3				4			
Atom	X	Y	Z	Atom	X	Y	Z
N(1)	0.7439	0.7827	0.7820	N(1)	0.3689	0.6048	0.5614
N(2)	0.4959	0.4222	0.8156	N(2)	0.6185	0.5286	0.7409
N(3)	0.3895	0.6294	0.8395	N(1)^{i}	0.6311	0.6048	0.9386
N(4)	0.2345	0.3517	0.9314	N(2)^{i}	0.3815	0.5286	0.7591
O(1)	0.5023	0.3918	0.9839	O(1)	0.4404	0.3602	0.6460
O(2)	0.5562	0.5614	0.9520	O(2)	0.5512	0.7797	0.7205
O(3)	0.9213	0.5537	0.8733	O(1)^{i}	0.5596	0.3602	0.8540
O(4)	0.2157	0.4437	0.7763	O(2)^{i}	0.4488	0.7797	0.7796

i –x+1,y,-z+3/2

When the bond lengths between Cd^{II} and donor atoms were examined, Cd-O bond lengths were observed to be the longest ones for both complexes. Besides, bond lengths around Cd^{II} centers were in compliance for both complexes. However, the only difference between coordination environments of metal centers in **3** and **4** was disappearance of symmetry around Ni^{II} and Cd^{II} centers because of existence of lattice water in **3**.

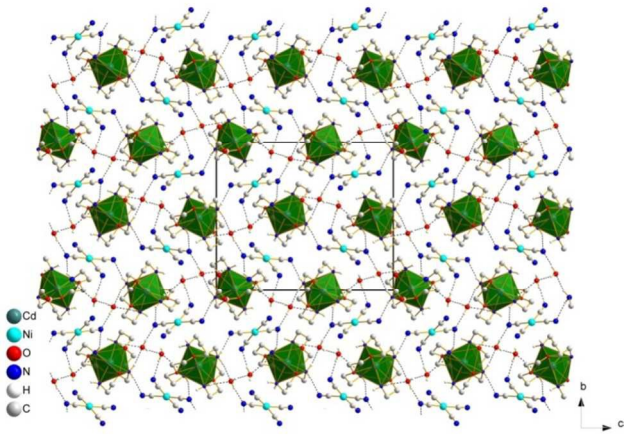

Fig 13 Packing of **3** from *a* direction. Green colored octahedrons represent the coordination around Cd atoms.

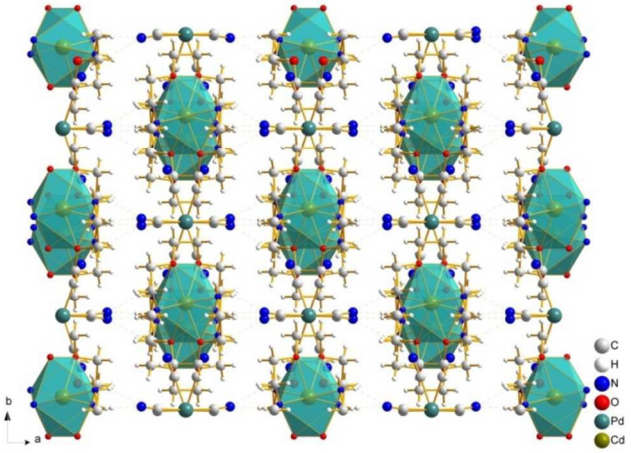

Fig 14 Packing of **4** along the *c* acis.

Both structures were stabilized by intermolecular *HBs* interactions and the important data related to *HBs* were depicted in Table 7. The existence of water molecules in **3** caused to form many *HBs* interactions in comparison with **4**. And, those water molecules formed the strongest HBs in the structure. When it comes to **4**, *HBs* had almost equal strength. Besides, oxygen atoms of *edbea* were observed not to participate in formation of *HBs* for both complexes.

The packing analysis of **3** showed the presence of a bi-layered structure where one layer is formed by complex cations and other by $[Ni^{II}(CN)_4]_n$ and $[OH_2]_n$ (Figure 15a). These cationic layers hosted the two dimensional sheets formed by *HBs* between the $Ni(CN)_4$ and water molecules. The constituent units in the anion-water sheets were held together by O1W-H2…N8, O2W-H3…N6 and O1W-H1W…O2W *HBs* (Table 7). These interactions between the anions and water molecules can be described in the form of a $R_8^8(28)$ graph set notation.[57] In addition, these sheets connected to each other by the *HBs* among complex cations, $Ni(CN)_4$ anions and water molecules. As a result of all these interactions, the packing of **3** shows a bi layered architecture and Cd centers between the two $Ni(CN)_4$…lattice waters layers are create *S*-shaped arrangement (Figure 15b) .

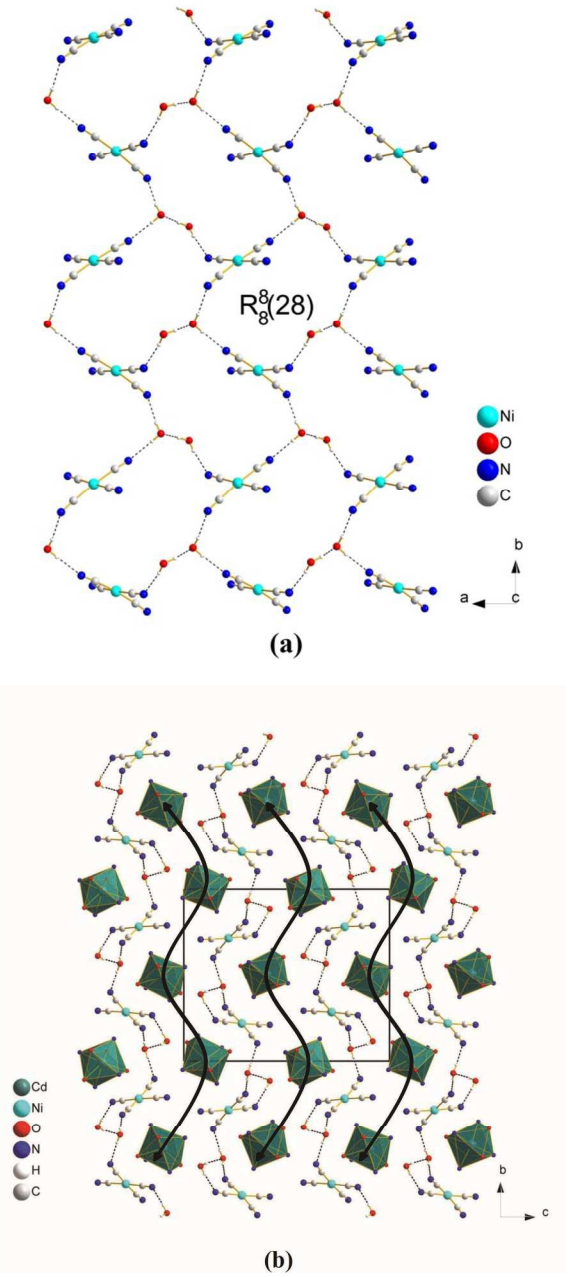

Fig 15 (a) Sheets of $Ni(CN)_4$ anions and water molecules showing the $R_8^8(28)$ graph set notation. **(b)** *S*-shaped arrangement of **3**.

Table 7 *HB*s data of **3** and **4**

		3		
	D–H	***H···A***	***D···A***	***D–H···A***
N(1)-H(1)···N(7)^{i}	0.90	2.26	3.091(5)	153
N(1)-H(1)···O(1W)^{ii}	0.90	2.36	3.206(5)	156
N(2)-H(2)···O(2W)^{iii}	0.90	2.53	3.358(5)	153
N(2)-H(2)···N(8)^{iv}	0.90	2.48	3.292(7)	151
O1W-H1WA···O2W	0.92	1.95	2.837 (4)	162
O(1W)-H(2)···N(8)	0.97	2.06	2.914(6)	146
O(2W)-H(3)···N(6)	0.97	2.49	2.859(6)	102
O(2W)-H(3)···N(2)^{v}	0.97	2.39	3.358(5)	172
N(4)-H(4)···O(1W)^{ii}	0.90	2.26	3.090(5)	152
		4		
	D–H	***H···A***	***D···A***	***D–H···A***
N(1)-H(1)…N(3)^{vi}	0.90	2.38	3.191(8)	149
N(2)-H(2)…N(3)^{vii}	0.90	2.26	3.128(6)	163
N(2)-H(2)…N(4)^{viii}	0.90	2.34	3.232(6)	171

(i) 3/2-x, -y, -1/2+z; (ii) 1/2+x, 1/2-y, -z; (iii) 2-x, -1/2+y, 1/2-z; (iv) 1+x, y, z; (v) 2-x, 1/2+y, 1/2-z; (vi) x-1/2,y-1/2,z; (vii) -x+3/2,y-1/2,-z+3/2; (viii) -x+1,-y+1,-z+1

Thermal Properties

Thermal curves for all complexes were comparatively shown in Figures 16 a and b. While **1** and **2** exhibited similar thermal stabilities according to DTG_{max} value of first decomposition stages, **3**, **4** and **5** had lower thermal stability in comparison with polymeric complexes, as expected (Table 8).

All complexes followed same usual multistage decomposition mechanism under nitrogen atmosphere. First, neutral *edbea* ligands left from structure for all complexes except for complex **3**. In thermal degradation of complex **3**, decomposition of *edbea* ligands was occured after evaporation of lattice waters. Then, all cyanido ligands decomposed for all complexes. Final products were metal or metal oxides in all situations. For complex **1**, thermal decomposition product included both metals (Ni and ZnO). Differently, remaining complexes left only one metal as residue (**2**→Ni, **3**→NiO, **4**→Pd, **5**→Pt) because of low boiling point of Cd metal.

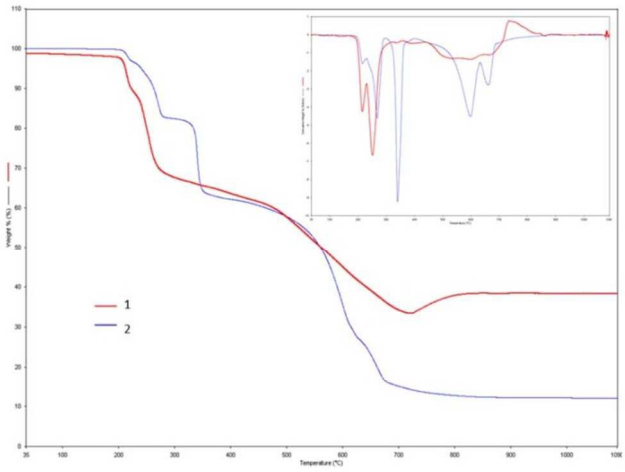

(a)

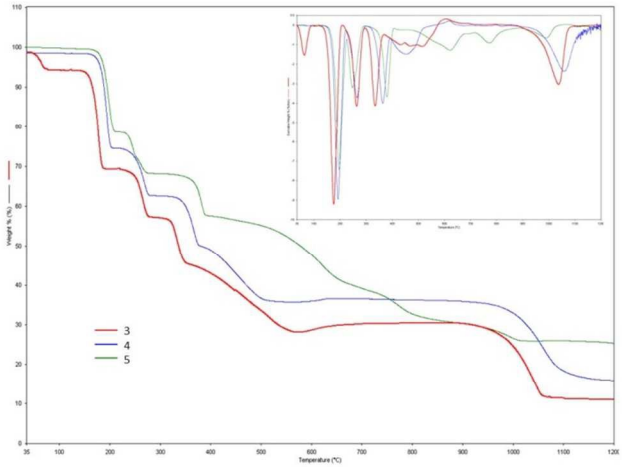

(b)

Fig 16 (a) Thermogravimetric curves of **1** and **2**. **(b)** Thermogravimetric curves of **3**-**5**.

Spectroscopic Properties

FT-IR spectroscopy is an important tool for characterization of cyanido-bridged complexes. Whether cyanido bridge forms or not can be determined by confirming split and shift in position of cyanido peak.[58] Two cyanido peaks (2164 and 2123 cm^{-1}) were observed for **1**, which has terminal and bridging cyanido ligands, differently from **2**, of which all cyanido ligands act as bridging ligand (2151 cm^{-1}). As to **3**, **4** and **5**, only one cyanido peak, at 2118 for **3**, 2127 for **4**, 2123 for **5**, appeared because of terminal ligand behavior of all cyanido

ligands. The peaks belonging to *edbea* ligands were approximately observed at expected wave numbers. Lattice water belonging to **3** appeared in the range of 3377-3695 cm^{-1} as overlapped with stretching vibration peaks of $-NH_2$ groups because of HBs.

CONCLUSIONS

Two cyanido-bridged polymeric complexes and three complex salt structures with *edbea*, which has not been used as a co-ligand for complex synthesis, frequently, were isolated. First, reactions of $[Ni(CN)_4]^{II}$ with Zn^{II} and Cd^{II} in the presence of *edbea* were carried out. *X*-ray single crystal studies pointed out that Zn^{II} formed only polymeric cyano-bridged complex under reaction conditions while both polymeric and monomeric structures were observed by using Cd^{II} center metal. This situation have conjured up that complex salt, which is crystallized first, is kinetically favored product and polymeric compound is thermodynamically favored product. Thermal analysis findings supported the idea, too. Kinetic product (**3**) had lower thermal stability than thermodynamic product (**2**). Thereon, the remaining members of group 10 were wondered what kind of complex structures to form and this time, Pd^{II} and Pt^{II} were used for synthesis of Cd complex instead of Ni^{II}. The results showed that Pd^{II} formed only salt structure but not polymeric complex probably because of not getting close of Pd^{II} ion with larger radius to Cd^{II} ion enough. **5** was suggested exhibiting salt structure like **4** based on the results of *FT-IR* spectra, elemental and thermal analysis. This suggestion was confirmed by illuminating *X*-ray powder structure of **5**. As a result, increase in metal ion radius of tetracyanidometallat^{II} fragment was concluded to facilitate ionic structure formation in comparison with polymeric complex formation when it comes to complexes with *edbea* co-ligand and Cd^{II} as second metal ion. However, the situation observed for complex **2** and **3** did not occur for other complex structures and only one kind of compound was obtained although the reaction mixtures were left to crystallization for weeks. On the other hand, similar thermal stability trend with **2** and **3** was observed for others and complexes with salt structures exhibited lower thermal stability compared to polymeric ones. Polymeric cyano-bridged complexes exhibited similar thermal decomposition stages in themselves, so did complexes with salt structure. An attractive aspect of this study was the coordination behavior of *edbea* ligand. While *edbea* ligand acted as tetradentate ligand by using all donor atoms in complex salts, same ligand coordinated to metal ions with nitrogen atoms for the purpose of bridge formation in an unusual manner in polymeric complexes. *Edbea* linked neighbor metal ions in cationic segment with different nitrogen atoms just like a suspension bridge in polymeric complexes.

EXPERIMENTAL

Materials and Methods.

$NiCl_2.6H_2O$, $ZnCl_2$, $CdSO_4.8/3H_2O$, $PdCl_2$, $PtCl_2$, KCN, ethanol and *edbea* were used as received.

Elemental analyses (C, H and N) were performed using a LECO CHNS-932 elemental analyzer. *IR* spectra were measured on a Jasco 430 *FT-IR* spectrometer using KBr pellets in the 4,000–400 cm^{-1} range. Thermogravimetric analyses were carried out on Perkin-Elmer Diamond *TG*/*DTA* Thermal Analysis instrument in nitrogen atmosphere with a heating rate of 10 $^oCmin^{-1}$ and 10 mg sample.

Synthesis of Complexes

Synthesis of 1. First, to ethanol (5 mL) and water (15 mL) solution of $NiCl_2.6H_2O$ (237.69 mg, 1 mmol) was added solid KCN (260.48 mg, 4 mmol) and yellow clear $K_2[Ni(CN)_4]$ solution formed. Then, $ZnCl_2$ solution in ethanol (136.32 mg, 1 mmol) was added to

this solution resulting in cream slurry. When *edbea* (148.20 mg, 1 mmol) was added to the obtained slurry under continuous stirring, a yellow clear solution formed within 5 min. The resulting solution was filtered and left to crystallization at room temperature. Yellow crystals suitable for *X*-ray analysis were obtained in a few weeks. The product was filtered off, washed with water and alcohol, and dried on air. [Zn(*edbea*)Ni(CN)$_4$] (**1**) Yield: 199.48 mg (0.53 mmol), 53%. Anal. Calc. for $C_{10}H_{16}N_6NiO_2Zn$: C, 31.91; H, 4.28; N, 22.33. Found: C, 31.79; H, 4.19; N, 21.58%. *IR* spectra (KBr disk; cm^{-1}) 3261,3234,3157 [υ(N–H)]; 2964,2945,2895,2877 [υ(C–H)]; 2164,2123 [υ(C≡N)]; 1618 [δ(N–H)]; 1061 [υ(C–O)].

Synthesis of 2 and 3. 2 was synthesized according to the procedure adopted for **1**, using $CdSO_4.8/3H_2O$ (257.11 mg, 1 mmol) rather than $ZnCl_2$. At the end of the reaction, two different crystals were obtained (**2** and **3**). First, big clear yellow crystals identified as salt were obtained within a few days. Then, small clear yellow crystals with polymeric structure were observed in a couple of weeks. [Cd(*edbea*)Ni(CN)$_4$] (**2**) Yield: 228.63 mg (0.54 mmol), 54%. Anal. Calc. for $C_{10}H_{16}CdN_6NiO_2$: C, 28.37; H, 3.81; N, 19.85. Found: C, 28.30; H, 3.21; N, 19.46%. *IR* spectra (KBr disk; cm^{-1}) 3356,3302 [υ(N–H)]; 2970,2931,2883,2831,2801 [υ(C–H)]; 2151 [υ(C≡N)]; 1588 [δ(N–H)]; 1062 [υ(C–O)]. [Cd(*edbea*)$_2$][Ni(CN)$_4$].2H$_2$O (**3**) Yield: 249.12 mg (0.41 mmol), 41%. Anal. Calc. for $C_{16}H_{36}CdN_8NiO_6$: C, 31.63; H, 5.97; N, 18.44. Found: C, 31.68; H, 5.70; N, 18.19%. *IR* spectra (KBr disk; cm^{-1}) 3695-3377 [υ(O–H)]; 3334,3298,3275,3186 [υ(N–H)]; 2966,2924,2916,2870 [υ(C–H)]; 2118 [υ(C≡N)]; 1597 [δ(N–H)]; 1043 [υ(C–O)].

Synthesis of 4 and 5. Solid KCN (260.48 mg, 4 mmol) was added to MCl_2 (177.33 mg, 1 mmol $PdCl_2$ for **4**; 265.98 mg, 1 mmol $PtCl_2$ for **5**) solution in ethanol/water (5/15). To the obtained clear tetracyanidometalat solution, $CdSO_4.8/3H_2O$ (257.11 mg, 1 mmol) was added and white slurry formed. Finally, when *edbea* (148.20 mg, 1 mmol) was added to the obtained slurry under continuous stirring, a colorless clear solution formed within 5 min. The resulting solution was filtered and left to crystallization at room temperature. Colorless crystal suitable for *X*-ray analysis was obtained for **4** in a few weeks. As to **5**, product was obtained as a white powder. The products were filtered off, washed with water and alcohol, and dried on air. [Cd(*edbea*)$_2$][Pd(CN)$_4$] (**4**) Yield: 514.03 mg (0.83 mmol), 83%. Anal. Calc. for $C_{16}H_{32}CdN_8O_4Pd$: C, 31.03; H, 5.21; N, 18.09. Found: C, 30.81; H, 5.07; N, 17.89%. *IR* spectra (KBr disk; cm^{-1}) 3350,3298,3275,3186 [υ(N–H)]; 2970,2922,2891,2879 [υ(C–H)]; 2127 [υ(C≡N)]; 1618 [δ(N–H)]; 1047 [υ(C–O)]. [Cd(*edbea*)$_2$][Pt(CN)$_4$] (**5**) Yield: 580.54 mg (0.82 mmol), 82%. Anal. Calc. for $C_{16}H_{32}CdN_8O_4Pt$: C, 27.14; H, 4.56; N, 15.83. Found: C, 26.27; H, 4.85; N, 15.61%. *IR* spectra (KBr disk; cm^{-1}) 3350,3298,3271,3186 [υ(N–H)]; 2970,2922,2891,2879 [υ(C–H)]; 2123 [υ(C≡N)]; 1576 [δ(N–H)]; 1047 [υ(C–O)].

***X*-Ray Crystallography.**

For the crystal structure determination of **1**-**4**, the single-crystals of complexes were used for data collection on a four-circle Rigaku R-AXIS RAPID-S diffractometer equipped with a two-dimensional area IP detector (**3**) and a STOE IPDS 2 diffractometer (**1**, **2** and **4**) at room temperature. The graphite-monochromatized MoKα radiation (λ= 0.71073 Å) and oscillation scans technique with Δω= 5^o for one image were used for data collection. The lattice parameters were determined by the least-squares method on the basis of all reflections with $F^2>2\sigma(F^2)$. Integration of the intensities, corrections for Lorentz and polarization effects and cell refinements were performed using Crystal-Clear (Rigaku/MSC Inc., 2005) software[59] (**3**) and X-AREA and X-RED32[60] (**1**, **2** and **4**). The structures were solved by direct methods SHELXS-97[61] and non-H atoms were refined by full-matrix least-squares method with anisotropic temperature factors SHELXL-

97.[61] H atoms were positioned geometrically and refined using a riding model. The final difference Fourier maps showed no peaks of chemical significance. Details of the final refinements were given in Table 9.

Structural characterization of **5** was performed using a Rigaku Smartlab high resolution X-ray diffractometer (XRD) with CuKα radiation (α= 1.540596 Å). Scan range, scan speed / duration time and ttep width were 2.0000-76.3028 deg, 0.0500 deg./min and 0.0004 deg., respectively. Single crystal data of **4** were used as initial atomic and lattice parameters. Pattern decomposition has been performed. Lattice, profile, Euler angles and base position of the fragments were refined by the Rietveld method using Rigaku PDXL XRD analysis software. When atomic coordinates were refined individually, bond lengths and angles deviated from their theoretical values and the moleculere structure broken apart. For this reason, atomic coordinates in Z-matrix were used during refinement. Atomic coordinates in Z-matrix were constrained by bond lengths and angles and refined as cationic and anionic molecular fragments. Refinement data for **5** were given in Table 10.

ACKNOWLEDGMENT

The work was support by the Scientific and Technical Research Council of Turkey (TUBITAK, Grant TBAG-104T205).

NOTES and REFERENCES

[a]Gaziosmanpaşa University, College of Art and Science, Department of Chemistry, 60240, Tokat, TURKEY; Tel: +90 356 252 1616 / 3066, 3058; ahmet.karadag@gop.edu.tr, ayseon@gmail.com

[b]Giresun University, Faculty of art and sciences, Department of Physics, 28100, Giresun, TURKEY; Tel: +90 454 310 1400; mustafa.serkan.soylu@giresun.edu.tr

[c]Ondokuzmayıs University, College of Art and Science, Department of Chemistry, 55139, Samsun, TURKEY; Tel: +90 362 312 1919 / 5455; oandac@gmail.com

Electronic Supplementary Information (ESI) available: [Cambridge Crystallographic Data Centre [CCDC ID: 971718 (**1**), 971719 (**2**), 977823 (**3**), and 764558 (**4**)]. Copies of the data can be obtained free of charge at www.ccdc.cam.ac.uk. or from the Cambridge Crystallographic Data Centre, 12 Union Road, Cambridge CB2 1EZ, UK (fax: +44-1223-336033 or e-mail: deposit@ccdc.cam.ac.uk)].

REFERENCES

1. G.A. Lawrance, in: D. Atwood, B. Crabtree, G. Meyer, D. Woollins (Eds.), *Introduction to Coordination Chemistry*, John Wiley & Sons, West Sussex, United Kingdom, 2010, **10**, 251-266.
2. R.J. Parker, L. Spiccia, K.J. Berry, G.D. Fallon, B.Moubaraki and K.S. Murray, *Chem. Commun*., 2001, **4**, 333-334.
3. Z.J. Zhong, H. Seino, Y. Mizobe, M. Hidai, A. Fujishima, S. Ohkoshi and K. Hashimoto, *J. Am. Chem. Soc*.,2000, **122**, 2952-2953.
4. F. Thétiot, S. Triki, J.S. Pala, C.J. Gómez-García and S. Golhen, *Chem. Commun.*,2002, **10**, 1078-1079.
5. E. Coronado, C.J. Gómez-García, A. Nuez, F.M. Romero, E. Rusanov and H. Stoeckli-Evans, *Inorg. Chem*., 2002,**41**, 4615-4617.
6. H.-Z. Kou, B.C. Zhou, S. Gao, D.-Z. Liao and R.-J. Wang, *Inorg. Chem*., 2003,**42**, 5604-5611.
7. M. Eddaoudi, H. Li and O.M. Yaghi, *J. Am. Chem. Soc*., 2000,**122**, 1391-1397.
8. S. Willemin, J. Larionova, R. Clérac, B. Donnadieu, B. Henner, X.F. Le Goff and C. Guérin, *Eur. J. Inorg. Chem.*,2003, **10**, 1866-1872.
9. P.S. Mukherjeee, T.K. Maji, T. Mallah, E. Zangrando, L. Randaccio and N.R. Chaudhuri, *Inorg. Chim.Acta*,2001, **315**, 249-253.
10. T. Senapati, C. Pichon, R. Ababei, C. Mathonière and R. Clérac, *Inorg. Chem.*,2012,**51**, 3796-3812.
11. J. Černák, M. Orendáč, I. Potočňák, J. Chomič, A. Orendáčová, J. Skoršepa and A. Feher, *Coord. Chem. Rev*.,2002, **224**, 51-66.
12. S. Tanase, M. Andruh, N. Stanica, C. Mathonière, G. Rombaut, S. Golhen and L. Ouahab, *Polyhedron*,2003, **22**, 1315-1320.
13. I.P.Y. Shek, W.-T. Wong, S. Gao and T.-C. Lau, *New J. Chem.*,2002, **26**, 1099-1101.
14. F. Bellouard, M. Clemente-León, E. Coronado, J. R. Galán-Mascarós, C. J. Gómez-García, F. Romero and K.R. Dunbar, *Eur. J. Inorg. Chem.*,2002, 1603-1606.
15. J.-Z. Gu, H.-Z. Kou, L. Jiang, T.-B.Lu and M.-Y. Tan, *Inorg.Chim.Acta*,2006, **359**, 2015-2022.

16. B.-Q. Ma, S. Gao, G. Su and G.-X. Xu, *Angew. Chem. Int. Ed*.,2001, **40**, 434-437.
17. A. Senocak, A. Karadag and E. Sahin, *J. Inorg. Organomet.Polym*.,2013, **23**, 1008-1014.
18. A. Hu, X. Chen, H. Zhou, Y. Chen and A. Yuan, *J. Coord. Chem*.,2013, **66**, 3241-3248.
19. D. Karaagac, G.S. Kurkcuoglu, O.Z. Yesilel and M. Tas, *Polyhedron*,2013, **62**, 286-292.
20. G.S. Kurkcuoglu, O.Z. Yesilel, I. Kavlak and O. Buyukgungor, *J. Molec. Struct*.,2009, **920**, 220-226.
21. A. Senocak, A. Karadag, Y. Yerli, O. Andac and E. Sahin, *J. Inorg. Organomet.Polym*., 2010, **20**, 628-635.
22. A. Senocak, *Synthesis, Characterization, Crystal Structure and Investigation of Magnetic Properties of New Bimetallic Cyano-Bridged Polymeric Complexes* (Doctoral Dissertation), Gaziosmanpasa University, 2010.
23. M. Salavati-Niasari and M. Bazarganipour, *Inorg. Chem. Commun*., 2006, **9**, 332-336.
24. M. Salavati-Niasari, *Polyhedron,* 2005, **24**, 1405-1409.
25. J. Černák, J. Lipkowski, I. Potočňák and A. Hudák, *Monatsh. Chem*.,2001, **132**, 193-202.
26. D. Ghoshal, A.K. Ghosh, T.K. Maji, J. Ribas, G. Mostafa, E. Zangrando and N.R. Chaudhuri, *Inorg. Chim.Acta*,2006, **359**, 593-602.
27. P.S. Mukherjeee, T.K. Maji, T. Mallah, E. Zangrando, L. Randaccio and N.R. Chaudhuri, *Inorg. Chim.Acta*,2001, **315**, 249-253.
28. A. Panja, *J. Coord. Chem*.,2011, **64**, 987-995.
29. Y. Li, L. Liu, D. Jia, J. Guo and R. Sheng, *J. Inorg. Organomet.Polym*.,2011, **21**, 254-260.
30. G.S. Kurkcuoglu, T. Hokelek, M. Aksel, O.Z. Yesilel and H. Dal, *J. Molec. Struct*.,2011, **21**, 602-610.
31. D. Zhang, L. Zhang, Z. Zhao and Z. Ni, *Synth. React. Inorg.Met.-Org. Nano-Met. Chem*.,2011, **41**, 1288-1292.
32. G. Kastas, H. Pasaoglu and B. Karabulut, *Polyhedron*,2011, **30**, 2599-2605.
33. A. Senocak, A. Karadag, E. Sahin and Y. Yerli, *J. Inorg. Organomet.Polym*.,2011, **21**, 438-449.
34. A. Karadag, A. Bulut, A. Senocak, I. Ucar and O. Buyukgungor, *J. Coord. Chem*.,2007, **60**, 2035-2044.
35. A. Senocak, A. Karadag, Y. Yerli, N. Gurbuz, I. Ozdemir and E. Sahin, *Polyhedron*,2013, **49**, 50-60.
36. E. Colacio, M. Ghazi, H. Stoeckli-Evans, F. Lloret, J.M. Moreno and C. Pérez, *Inorg. Chem.*,2001, **40**,4876-4883.
37. I. Caylı, G.S. Kurkcuoglu, O.Z. Yesilel, O. Sahin and O. Buyukgungor,*Polyhedron*,2012, **31**, 386-394.
38. A. Karadag, I. Onal, A. Senocak, I. Ucar, A. Bulut and O. Buyukgungor, *Polyhedron*,2008, **27**, 223-231.
39. G.A. Jeffrey, H. Maluszynska andJ.Mitra, *Int. J. Biol. Macromol*.,1985, **7**, 336-348.
40. V.A. Blatov, A.P. Shevchenko, D.M. Proserpio, *Cryst. Growth Des.*, 2014, **14**, 3576-3586.
41. A.L. Spek, PLATON, A Multipurpose Crystallographic Tool, Utrecht University, Utrecht, The Netherlands, 2001.
42. G.S. Kurkcuoglu, T. Hokelek, O.Z. Yesilel and S. Aksay, *Struct. Chem*.,2008, **19**, 493-499.
43. A. Karadag, H. Pasaoglu, G. Kastas and O. Buyukgungor, *ActaCryst*.,2004, **C60**, m581-m583.
44. G.S. Kurkcuoglu, O.Z. Yesilel, I. KavlakandO. Buyukgungor, *J. Inorg. Organomet.Polym*.,2009, **19**, 539-548.
45. R. Wang, H. Xia and L.B. Nie, *Russ. J. Coord. Chem.,*2009, **35**, 720-722.
46. X. Chen, P. Yang, S.-L.Ma, S. Ren, M.-Y.Tang, Y. Yang, Z.-J.Guo and L.-Z. Liu, *J. Struct. Chem*.,2009, **50**, 495-499.
47. G.S. Kurkcuoglu, O.Z. Yesilel, I. KavlakandO. Buyukgungor, *Z. Anorg. Allg. Chem*.,2009, **635**, 175-178.
48. S.-Z. Zhan, D.-S.Sun, J.-G.Wang, J.-Y.Zhou, A.-Q.Liang and J.-Y. Su, *J. Coord. Chem*.,2008, **61**, 550-562.
49. S.C. Manna, J. Ribas, E. Zangrando and N.R. Chaudhuri, *Polyhedron*,2007, **26**, 3189-3198.
50. J. Černak, J. Skoršepa, K.A. Abboud, M.W. Meisel, M. Orendač, A. Orendačova and A. Feher, *Inorg. Chim.Acta*,2001, **326**, 3-8.
51. J. Kuchar, J. Černak and K.A. Abboud, *ActaCryst*.,2004, **C60**, m492-m494.
52. A.O. Legendre, A.E. Mauro, M.A.R. Oliveira and M.T.P. Gambardella, *Inorg. Chem. Commun*.,2008, **11**, 896-898.
53. J.K. Burdett, R. Hoffmann and R.C. Fay, *Inorg. Chem*.,1978, **17**,2553-2568.
54. E.L. Muetterties and C.M. Wright, *Q. Rev. Chem. Soc*.,1967, **21**, 109-194.
55. C.W. Haigh, *Polyhedron*,1995, **14**, 2871-2878.
56. J. Xu, E. Radkov, M. Ziegler and K.N. Raymond, *Inorg. Chem*.,2000, **39**,4156-4164.
57. J. Bernstein, R.E. Davis, L. Shimoni and N.L. Chang, *Angew. Chem. Int. Ed. Engl.*,1995, **34**, 1555-1573.
58. K. Nakamato, *Infrared and Raman Spectra of Inorganic and Coordination Compounds* Part B, John Wiley & Sons, Inc., Hoboken, New Jersey, 2009, 110.
59. Rigaku/MSC, Inc., 9009 New Trails Drive. The Woodlands, TX, USA, 2005.
60. Stoe&Cie, X-AREA (Version 1.18) and X-RED32 (Version 1.04), Stoe&Cie, Darmstadt, Germany, 2002.
61. G.M. Sheldrick, *SHELXS97 and SHELXL97*,University of Göttingen, Germany, 1997.

Table 8 Thermoanalytical data of **1-5**

Complex	Stage	Temperature Range (°C)	DTG_{max}	Mass Loss Δm (%)		Total Mass Loss Δm (%)		Residue	
				Found	Calcd.	Found	Calcd.	Found	Calcd.
1	1	161-232	216	10.35		10.35		89.65	
	2	232-396	252	24.51	53.25	34.86	53.25	65.14	46.75
	3	396-591	522	17.52		52.8		47.62	
	4	591-646	597	6.65	6.92	59.03	60.17	40.97	39.83
	5	646-722	676	6.21	6.92	65.24	67.09	34.76	32.91
	6	722-836	819	+4.94	+4.25	60.30	62.84	39.70	37.16 Ni+ZnO
2	1	177-230	216	3.42		3.42		96.58	
	2	230-299	270	14.00	41.15	17.42	41.15	82.58	58.85
	3	299-485	341	23.59		41.01		58.99	
	4	485-633	598	32.31	45.02	73.32	86.17	26.68	13.83 Ni
	5	633-783	661	13.61		86.93		13.07	
3	1	39-110	63	4,54	4,51	4,54	4,51	95,46	95,49
	2	110-209	176	24,95	24,76	29,49	29,27	70,51	70,73
	3	209-296	263	12,15	24,76	41,64	54,03	58,36	45,97
	4	296-368	334	12,23		53,87		46,13	
	5	368-577	516	16,79	17,39	70,66	71,42	29,34	28,58
	6	577-729	666	+2,21	+2,67	68,45	68,75	31,55	31,25
	7	891-1076	1037	18,91	18,78	87,36	87,53	12,64	12,47 NiO
4	1	143-224	193	23,94	23,93	23,94	23,93	76,06	76,07
	2	224-300	262	11,88	23,93	35,82	47,86	64,18	52,14
	3	300-383	367	13,04		48,86		51,04	
	4	383-649	469	13,50	12,60	62,36	60,46	37,64	39,54
	5	838-1273	1056	21,42	22,35	83,78	82,81	16,22	17,19 Pd
5	1	160-223	197	20,89	20,93	20,89	20,93	79,11	79,07
	2	223-298	247	10,45	20,93	31,34	41,86	68,66	58,14
	3	298-402	380	10,63		41,97		58,03	
	4	402-702	623	18,46		60,43		39,57	
	5	702-882	773	8,47	30,58	68,90	72,44	31,10	27,56 Pt
	6	882-1010	994	4,49		73,39		26,61	

Table 9 Crystal data and structure refinement for **1**-**4**

	1	**2**	**3**	**4**
Empirical formula	$C_{10}H_{16}N_6O_2NiZn$	$C_{10}H_{16}N_6O_2NiCd$	$C_{16}H_{36}N_8O_6NiCd$	$C_{16}H_{32}N_8O_4PdCd$
Crystal color	Yellow	Yellow	Yellow	Colorless
Fw	376.36	423.38	607.60	619.33
Crystal system	Orthorhombic	Monoclinic	Orthorhombic	Monoclinic
Space Group	P*bcn*	C2/c	$P2_12_12_1$	C2/c
Crystal size (mm^3)	0.720 x 0.527 x 0.320	0.610 x 0.517 x 0.410	0.23 x 0.12 x 0.10	0.560 x 0.463 x 0.320
Z	4	4	4	4
a (Å)	11.4558(6)	10.8081(5)	9.6650(5)	18.5700(14)
b (Å)	8.9466(6)	10.4606(4)	14.9620(5)	10.3191(7)
c (Å)	14.7706(7)	14.2364(5)	17.9210(5)	17.2851(14)
α (°)	90.00	90.00	90.00	90.00
β (°)	90.00	107.209(3)	90.00	133.390(5)
γ (°)	90.00	90.00	90.00	90.00
V ($Å^3$)	1513.84(15)	1537.50(10)	2591.8(2)	2407.0(4)
Abs. correction	Integration	Integration	Integration	Integration
ρ_{calcd} (g cm^{-3})	1.65	1.83	1.56	1.71
μ (mm^{-1})	2.84	2.62	1.59	2.76
F(000)	768	840	1248	1240
θ range (deg)	1.78-28.00	1.50-28.04	2.40-26.40	2.33-27.77
Limiting indices	$-12 \le h \le 14$ $-9 \le k \le 11$ $-19 \le l \le 19$	$-14 \le h \le 14$ $-13 \le k \le 13$ $-16 \le l \le 18$	$-12 \le h \le 12$ $-18 \le k \le 18$ $-22 \le l \le 22$	$-24 \le h \le 24$ $-13 \le k \le 13$ $-22 \le l \le 22$
Reflns collected	12350	30074	55476	17480
Independent reflns	7963	12464	5323	2784
T min/max	0.2128/0.4714	0.3182/0.4041	0.8263/0.8532	0.2215/0.3948
Goodness-of-fit on F^2	1.069	1.186	1.111	1.100
R1/wR2 [$F^2 > 2\sigma(F^2)$]	0.0349/0.0823	0.0204/0.0458	0.0307/0.0680	0.0403/0.0970
Data / restrains / parameters	1738/0/94	1772/0/88	5323/0/290	2784/0/138
Largest diff. peak / hole ($Å^{-3}$)	0.698/-0.391	0.554/-0.605	0.323/-0.378	0.687/-0.741
Flack Parameter*	-	-	0.021(16)	-

*: H.D. Flack, *Acta Cryst.* 1983, **A39**, 876-881.

Table 10 Crystal and structure refinement data for **5**

Empirical formula	$C_{16}H_{32}N_8O_4PtCd$
Crystal color	Colorless
Fw	707.97
Crystal system	Monoclinic
Space Group	C2/c
Z	4
a (Å)	18.6168(3)
b (Å)	10.33190(14)
c (Å)	17.3340(2)
α (°)	90.00
β (°)	133.6080(5)
γ (°)	90.00
V (Å^3)	2414.16(6)
Rwp	13.68
Rp	9.91
Re	9.95
S	1.3746
Chi^2	1.8895
Maximum shift/e.s.d.	1.911
Background Function name	B-spline
Peak shift Function name	Shift axial displacement
Scale factor s	12.309(19)
FWHM U	0.273(4)
V	-0.0972(14)
W	0.01556(15)
Asym. Factor A0	0.501(13)
A1	1.23(5)
Decay rate factor etaL0/mL0	1.327(10)
etaL1/mL1	-0.04(2)
etaL2/mL2	0.0000
etaH0/mH0	0.471(5)
etaH1/mH1	0.64(3)
etaH2/mH2	0.0000

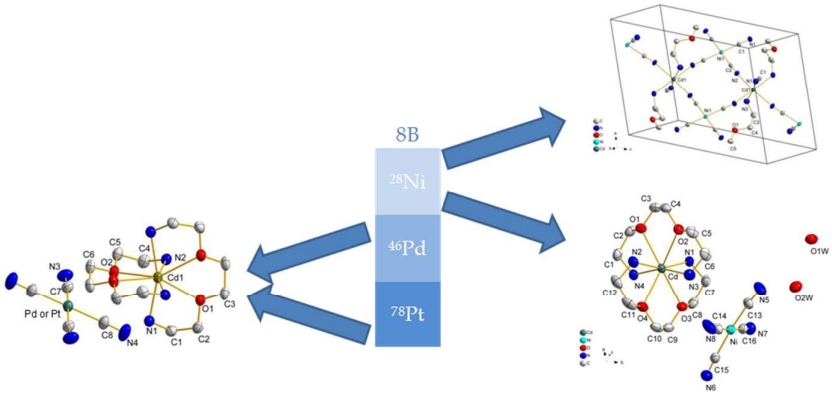

Polymeric complexes exhibiting interesting suspension bridge type binding via 2,2′-(ethylenedioxy)bis(ethylamine) and dissimilarity in complex formation behavior of 8B group members were revealed.